Pratt & Whitney Thermal Barrier Coating Development

Mladen F. Trubelja (trubelm@pweh.com; 860-565-0249)
David M. Nissley (nissledm@pweh.com; 860-565-5843)
Norman S. Bornstein (bornstns@utrc.utc.com; 860-610-7487)*
Jeanine T. D. Marcin (marcinj@pweh.com; 860-565-4784)
Pratt & Whitney, 400 Main Street, East Hartford, CT 06108
*United Technologies Research Center, 411 Silver Lane, East Hartford, CT 06108

Introduction

Over the past two decades, substantial advances have been made in the use of thermal barrier coatings (TBCs) to protect nickel-based superalloys against the deleterious effects of high-temperature turbine environments. TBC use results in considerable improvements in durability of hot-section turbine components, as well as in an increase of gas turbine thermodynamic efficiency. The TBCs typically consist of a ceramic insulating layer deposited on the substrate with an intervening metallic layer (bond coat), which imparts oxidation protection to the substrate, and provides a surface to which the ceramic layer can adhere.

Even though TBCs have enjoyed success primarily in revenue-generating aircraft engine service, more recent years have seen an increasingly significant role for the TBCs in industrial gas turbine (IGT) applications. However, the IGT operating profiles are long, less cyclic, with fewer transients compared with those for aircraft gas turbine engines. Therefore, creep, rather than thermal fatigue is the primary life-limiting mechanism for hot-section components. In addition, the industrial engine operates in a harsher, less forgiving environment than an aero-engine because of the potential presence of the contaminants continuously ingested from the engine surroundings.

In this program, TBCs are being developed to meet the Advanced Turbine Systems (ATS) objectives of providing thermal insulation and imparting the oxidation and hot-corrosion resistance needed to hold the turbine component temperatures to the limits required for 25,000-hour creep life. In this paper, progress is reviewed in understanding the operational envelope, and defining the necessary chemical, mechanical, and physical materials properties to meet the ATS goals. Surface morphologies observed on the service-run IGT components are compared to the results of the laboratory experiments. Furthermore, insight is provided into the relevant properties of two promising candidate materials (a ceramic and a bond coat). Finally, demonstrated operating capabilities of the unique thermal gradient burner rig are summarized.

Objectives and Approach

The objective of the ATS Program is to develop ultra-highly efficient, environmentally superior, and cost-competitive gas turbine systems. The ATS Program specifies combustor and blade creep life of about 25,000 h, which roughly corresponds to the period between inspections.[1, 2] In addition to oxidation and, to a lesser extent, thermal cycling, this extended overhaul interval, which is approximately five times longer than typical intervals for aircraft turbines, introduces hot corrosion and erosion as critical elements affecting durability. The durability and performance demands of ATS can be achieved by appropriate reductions of metal temperatures to retain the structural properties of the substrate alloys. This can be accomplished by applying TBCs to the substrate.

Consequently, the overall objective of the Pratt & Whitney program is to develop TBCs for land-based gas turbines, to assist in successfully and economically meeting the ATS goals of increased operating efficiencies. The TBC development objectives are as follows:[3]

i. Ensure TBC stability in thermal, oxidative, corrosive, and erosive IGT environment,
ii. Use both air-plasma sprayed (APS) and electron-beam physically vapor deposited (EB-PVD) coatings,
iii. Meet 25,000 h creep life for blade and combustor applications, and
iv. Provide optimized thickness to hold temperatures commensurate with creep life and leading edge erosion.

These objectives are being met in the current program using the following approach:

i. Selection of ceramic and bond coat systems,
ii. Screening through critical gradient and isothermal burner rig, as well as controlled-atmosphere furnace tests,
iii. Developing and validating an analytical model for durability prediction,
iv. Developing a TBC manufacturing process, and
v. Developing the techniques for repair, maintenance, and inspection of TBCs.

Project Description

The Project consists of the following four phases:

- Phase I: Program Plan,
- Phase II: Development,
- Phase III: Selected Hot Section Specimens—Bench Tests, and
- Phase IV: Selected Airfoil Testing in Product Line Gas Turbine (currently an option).

After successful completion of Phase I early in the Program, the development and testing of candidate ceramic and bond coat materials are now well under way in Phase II (shown

schematically in Figure 1). Along the critical path of the Program, the ceramics are being screened through gradient and nongradient cyclic burner rig tests (A1 and A2,

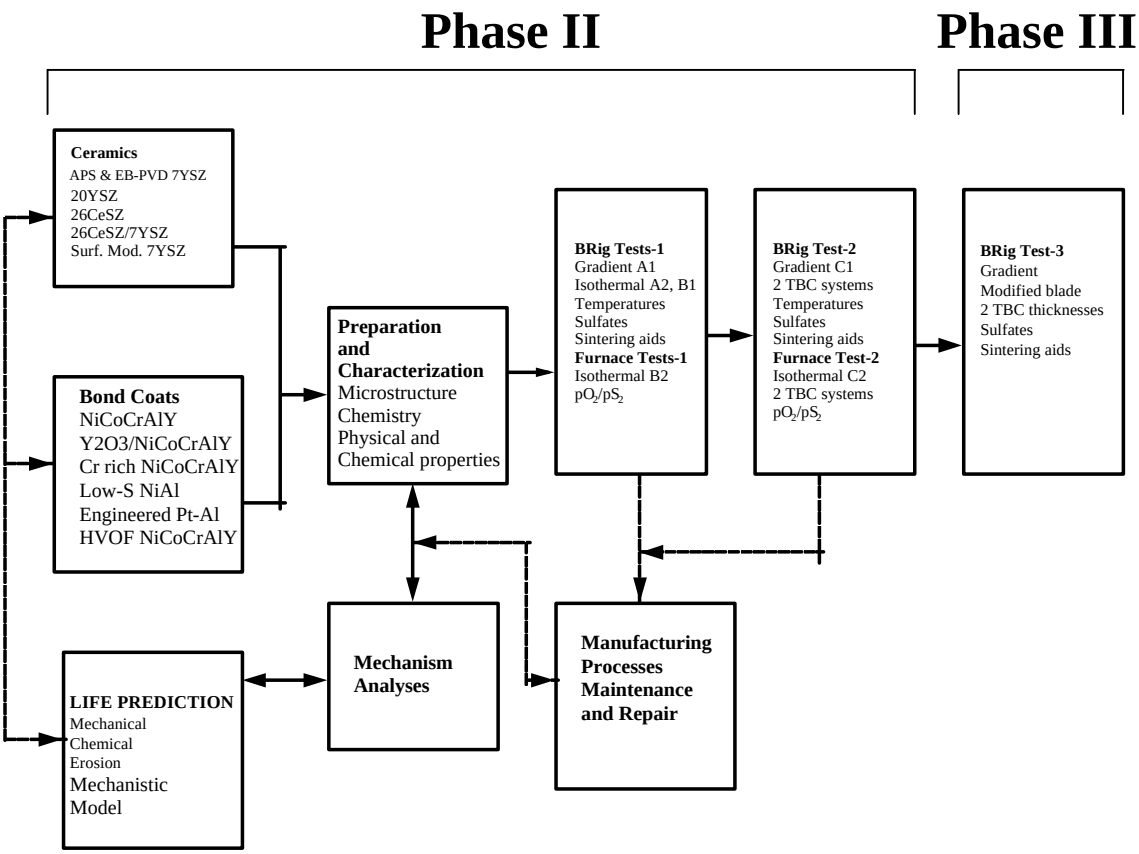

Figure 1. Phase II and III flow chart.

respectively), with and without the presence of corrodents and sintering agents on the specimen surfaces. Bond coats are being evaluated through nongradient cyclic burner rig tests with the corrodents and sintering agents applied onto the specimen surfaces (B1 tests), as well as through isothermal furnace exposure tests conducted in a controlled sulfur-containing atmosphere (B2 tests).

One (or two) down-selected ceramics will then be combined with two (or one) down-selected bond coats to form two candidate TBC systems, which are to be tested in a cyclic gradient burner rig test (C1), as well as an isothermal controlled-atmosphere furnace test (C2), to yield the final down-selected TBC system. This system will then be applied onto a turbine blade and bench-tested in a gradient cyclic burner rig test (Phase III; see Figure 1) in the presence of corrodents and sintering agents. The nature and chemical compositions of the corrodents and sintering agents used in testing are described in the following section.

Accomplishments and Benefits

Hot Corrosion Mechanism(s): Field vs *Laboratory Observations*

Hot corrosion is the term that describes accelerated oxidation of high-temperature materials associated with the formation of corrosive deposits.[4] Sulfidation corrosion, a form of hot corrosion, is related to the deposition of alkali-rich sulfate salts. The name is derived from the presence of sulfur in the scale, or the precipitation of sulfur-rich phases in an affected zone that separates the scale from the matrix.

The principal corrosive compound associated with sulfidation corrosion is sodium sulfate. In addition, the salt deposits detected on IGT blade surfaces include the sulfates of potassium, calcium and magnesium. The principal source of sulfate corrodents is sea salt, which is present in the air and has the potential to ingress an industrial engine. In general, as the sea-salt droplets pass through the low- and high-pressure compressor, the concentration of the salts increases as water evaporates from the surface, and the salts selectively precipitate on the high-pressure compressor in the reverse order of their respective water solubilities. Subsequently, fragments of the deposits may break off intermittently from the compressor, enter the turbine section, and deposit onto the turbine blades by impaction.[3]

Surface morphology observations on service-run IGT blades examined in this program (an example is shown in Figure 2a) indicate evidence of simultaneous presence of both Type I and Type II hot corrosion on a single component.[4] The two forms of sulfidation corrosion are distinguished principally by the metallographic appearance. Type I (high-temperature corrosion), characterized by a broad-front attack, with internal chromium-rich sulfides in the zone depleted of reactive elements (Figure 2b), occurs at temperatures of 800°C (1472°F) and above. Type II (low-temperature corrosion), exhibiting a pitting attack, with little or no presence of internal sulfides or alloy depleted zone (Figure 2c), is primarily observed in the temperature range between 650° and 775°C (1202° and 1427°F). In this program, both surface morphologies were duplicated in the laboratory experiments by applying thin films (~0.5 mg/cm^2) of the low-melting eutectic mixtures from the ternary system $MgSO_4$–Na_2SO_4–$CaSO_4$ (with minor additions of K_2SO_4) onto the surfaces of various turbine component materials, and exposing them to the temperatures of 750°C (1382°F) and 900°C (1652°F) (Figure 3).[4]

In addition to the corrosive sulfate mixtures discussed above, the oxides of silicon and iron are commonly detected in engine-run hot section components. The principal source of iron oxides is the structural components that are made of steel, whereas silica is the principal constituent of the indigeneous dusts associated with both industrial and rural areas. It is interesting to note that in ceramic-coated, service-run hot-section components, fine particles rich in chromium and sulfur are still present near the bond coat/ceramic interface (Figure 4). Furthermore, in the spalled regions of the ceramic, significant amounts of monoclinic zirconia are detected, indicating phase-destabilization effects of the contaminant mixtures on partially stabilized zirconia. Finally, the mixtures of iron

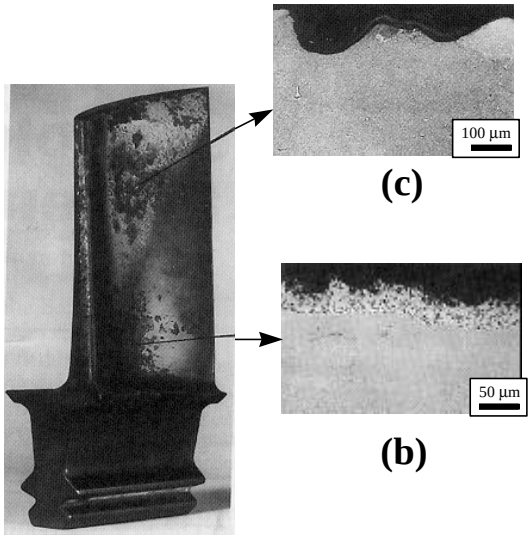

Figure 2. Service-run IGT blade (a) showing simultaneous presence of Type I (b) and Type II (c) hot corrosion.

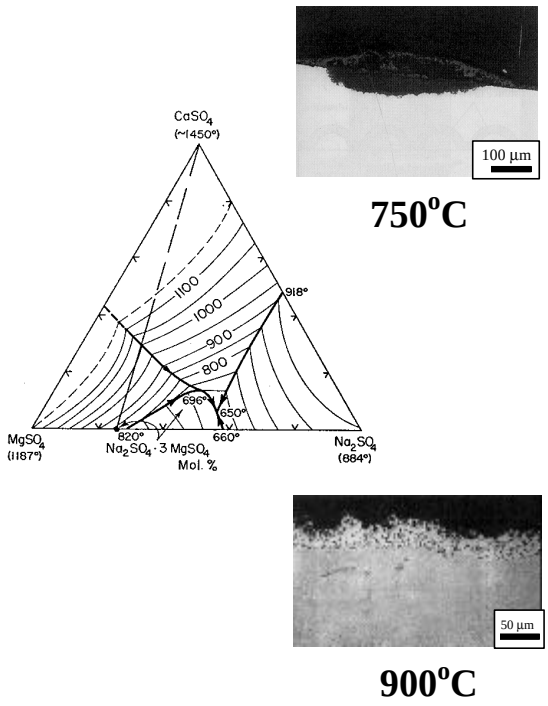

Figure 3. Microstructures of a turbine component material exposed to a ternary eutectic mixture, duplicating field-service observations shown in Figure 2.

Figure 4. Microstructure of a service-run TBC-coated hot-section component showing the presence of fine chromium and sulfur-rich particles near the bond coat/ceramic interface.

oxides and silica are powerful sintering agents that can interact with zirconia, resulting in densification, tensile residual stresses, and shrinkage cracks leading to premature failure.[3]

In this program, the ceramic interactions with the contaminants commonly observed in the field were studied in the laboratory by isothermally exposing the surface of an electron-beam physically vapor deposited (EB-PVD) ceramic to the mixtures of corrodent sulfates and sintering agents at 1204°C (2200°F) for 16 h. The exposure resulted in considerable penetration of the contaminants into the intercolumnar spaces of the coating (Figure 5). In addition, a thin, potentially damaging reaction zone between the PVD tips

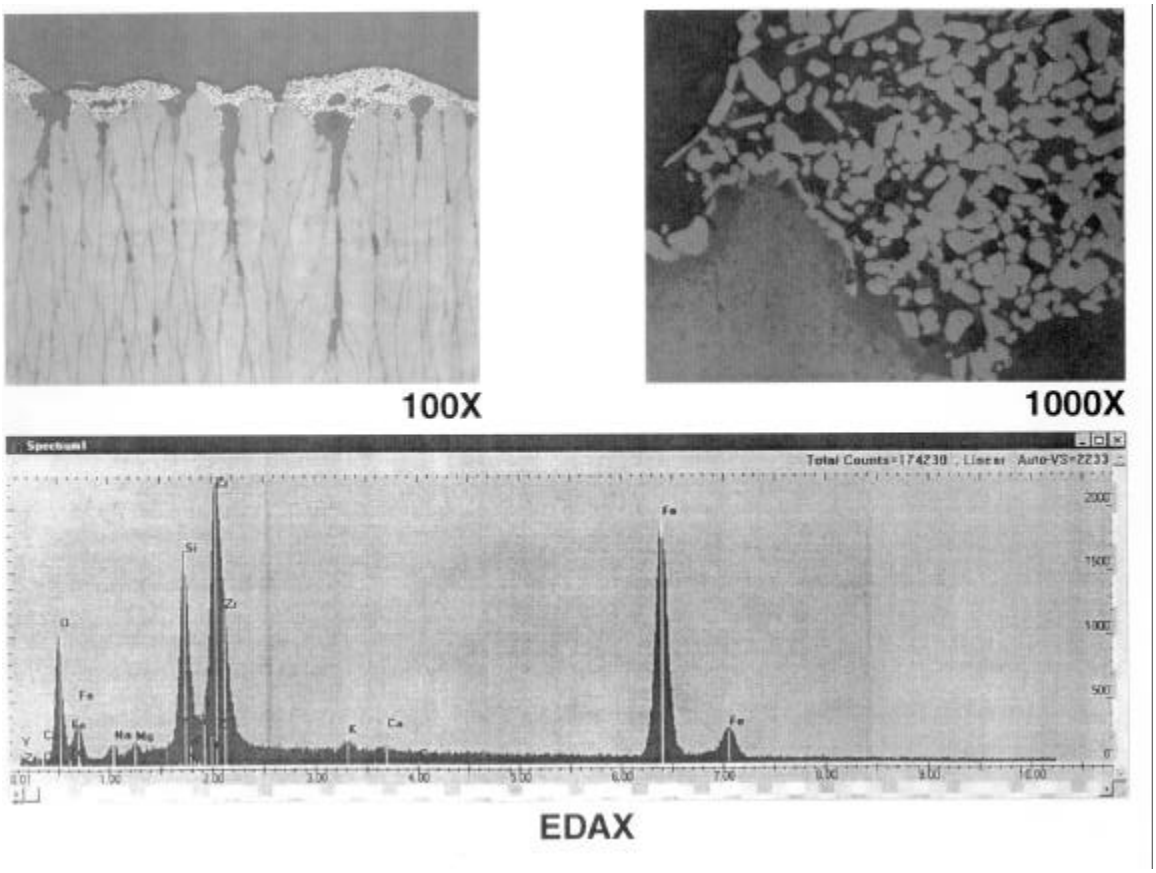

Figure 5. Microstructure and EDS analysis results for the reaction zone formed by exposing the EB-PVD 7YSZ ceramic to the corrodents and sintering agents for 16 h at 1204°C.

and the contaminants was clearly identifiable. Note, as well, that the energy-dispersive spectroscopic (EDS) analysis of this reaction zone indicated the presence of all the contaminants, with the exception of sulfur, suggesting that thermal decomposition of the sulfates had occurred. Even more dramatic effects were observed after a longer-term (1000-hour) isothermal exposure of an EB-PVD ceramic-coated specimen to a somewhat lower temperature (1038°C or 1900°F). This experiment (Figure 6) resulted in complete

penetration of the contaminants to the bond coat; the formation of porosity and major crack propagation within the bond coat; and, ultimately, the spallation of the entire TBC.

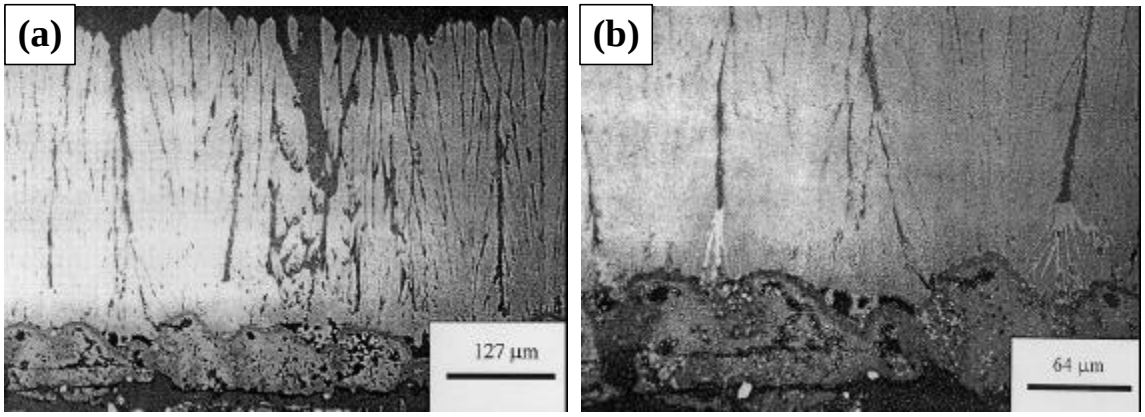

Figure 6. Microstructure at 200× (a) and 400× (b) of an EB-PVD 7YSZ ceramic, showing contaminant infiltration to the bond coat after exposure to 1038°C for 1000 h.

Based on the results of the field observations and laboratory tests presented above, the TBC degradation mechanism(s) believed to be relevant to ATS can be summarized in the following manner (Figure 7): Corrodent salt mixtures ingested at random from an

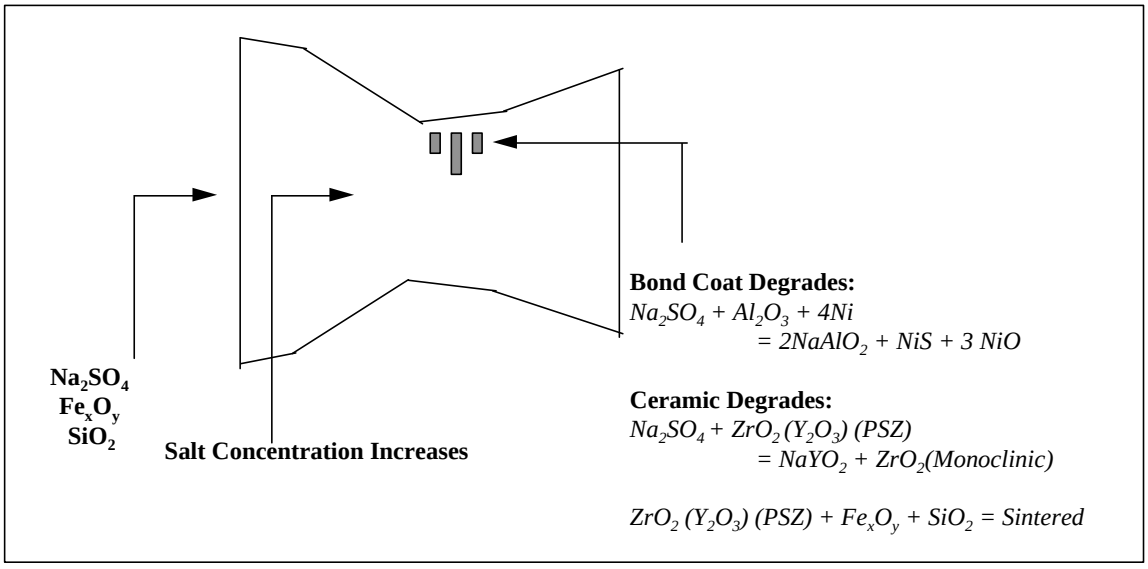

Figure 7. Schematic summary of TBC degradation mechanisms relevant to ATS.

engine's surroundings are concentrated in the compressor section and deposited onto the high-pressure compressor blades, intermittently detached and transferred into the turbine section, and subsequently deposited by impaction onto the turbine blades. Sintering agent mixtures are ingested into the engine, and subsequently deposited directly into the turbine

section. Both the bond coat and ceramic are affected by the corroding sulfates, causing bond coat sulfidation corrosion and ceramic phase destabilization. Iron oxides and silica, on the other hand, promote ceramic sintering, leading to spallation due to densification, tensile residual stresses, and shrinkage.

TBC Test Results

Current Pratt & Whitney flight-engine TBC experience and an extensive existing data base of short-cycle spallation-life test results clearly indicate that, among the ceramics listed in Figure 1, the only viable state-of-the-art candidate for potential IGT blade applications is the EB-PVD 7 wt% yttria-stabilized zirconia (7YSZ). However, it was shown above that the EB-PVD 7YSZ material alone is prone to infiltration by the contaminants present in an industrial engine environment (Figures 5 and 6). Therefore, in this program, the surface of EB-PVD 7YSZ ceramic was modified with an additional thin ceramic layer to seal the intercolumnar spaces against the penetration of corrodents and sintering agents (Figure 8).

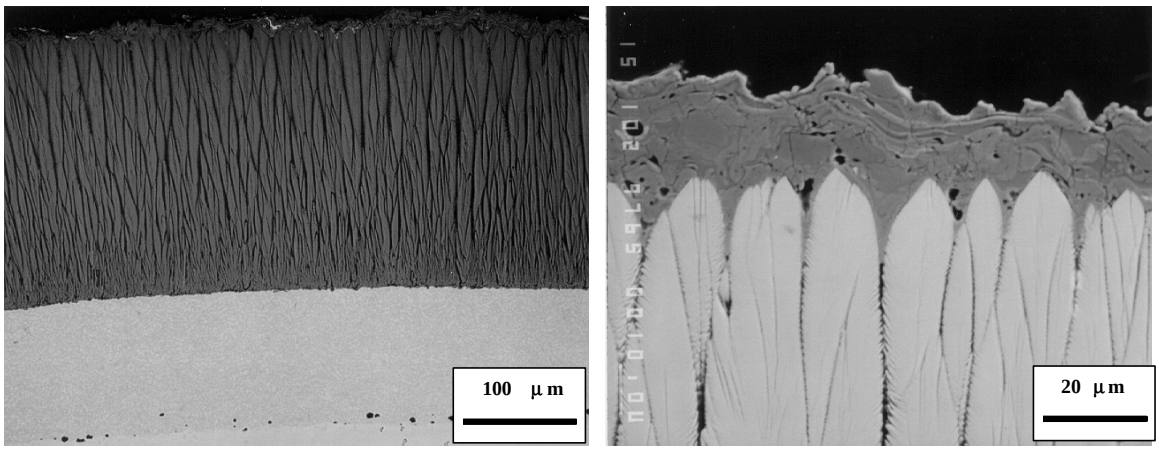

Figure 8. Typical as-coated microstructure of a surface-modified EB-PVD 7YSZ specimen.

This new material was then evaluated in cyclic oxidation and erosion tests against several other ceramic candidates. The results of the cyclic oxidation tests are shown in Figure 9. The test was conducted in a standard burner rig at 1149°C (2100°F) with a 1-hour thermal cycle. The results suggest that the surface-modified and standard EB-PVD 7YSZ coatings have an equivalent spallation life. In addition, both candidate materials are at least an order of magnitude superior in spallation life to the plasma-sprayed ceramics, which are, at present, most commonly used on vane platforms and transition ducts of industrial engines.

Macroscopic examination of a failed specimen coated with the surface-modified PVD ceramic suggests that the failure occurred by spallation in the area between the hot zone on the trailing edge of the specimen (the view shown in Figure 10a), and the flame

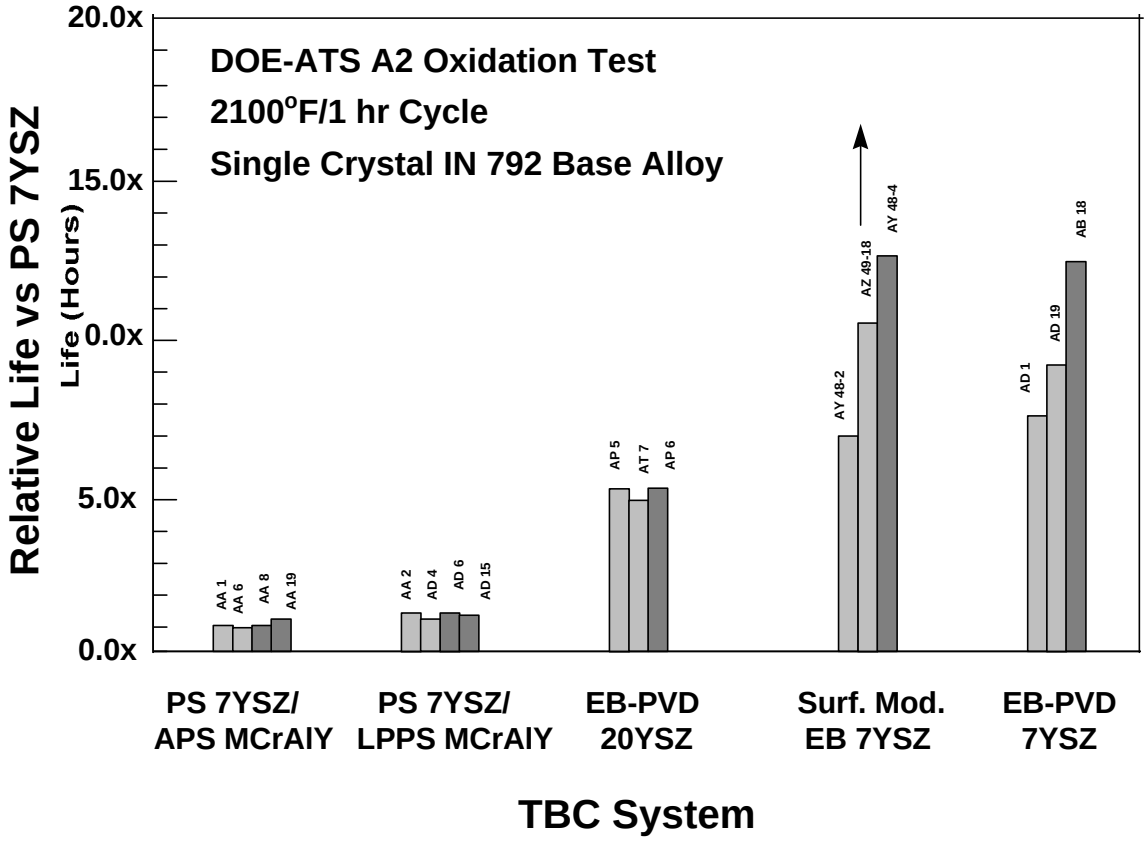

Figure 9. Results of a standard oxidation burner rig test for several candidate ceramics. Arrow indicates an unfailed specimen.

impingement zone on the leading edge of the specimen. Further examination of Figure 10a, and a cross section view obtained from the hot zone on the specimen trailing edge (Figure 10b) both indicate that the ceramic spallation is accompanied by severe pitting of the bond coat. The post-test view of the cross section further shows that the ceramic layer is completely removed, while the bond coat is significantly depleted of the β-phase near the exposed surface, as well as near the interface with the base alloy. A scanning electron microscopy (SEM) (Figure 10c) and EDS (Figure 10d) examination of the critical area on the surface of the failed specimen indicates that the failure occurred primarily within the thermally grown oxide layer (note a strong Al peak in the EDS spectrum).

Several TBC specimens, fully or partially spalled in the cyclic oxidation test, were also examined by electronic holography as part of the nondestructive evaluation effort (an example of a failed APS-coated specimen is shown in Figure 11). Even though no evidence of spallation is observed on the trailing edge of the specimen (Figure 11a), electronic holography image (Figure 11b) clearly indicates that TBC delamination has occurred. This is confirmed by an optical microscopy examination of a cross section

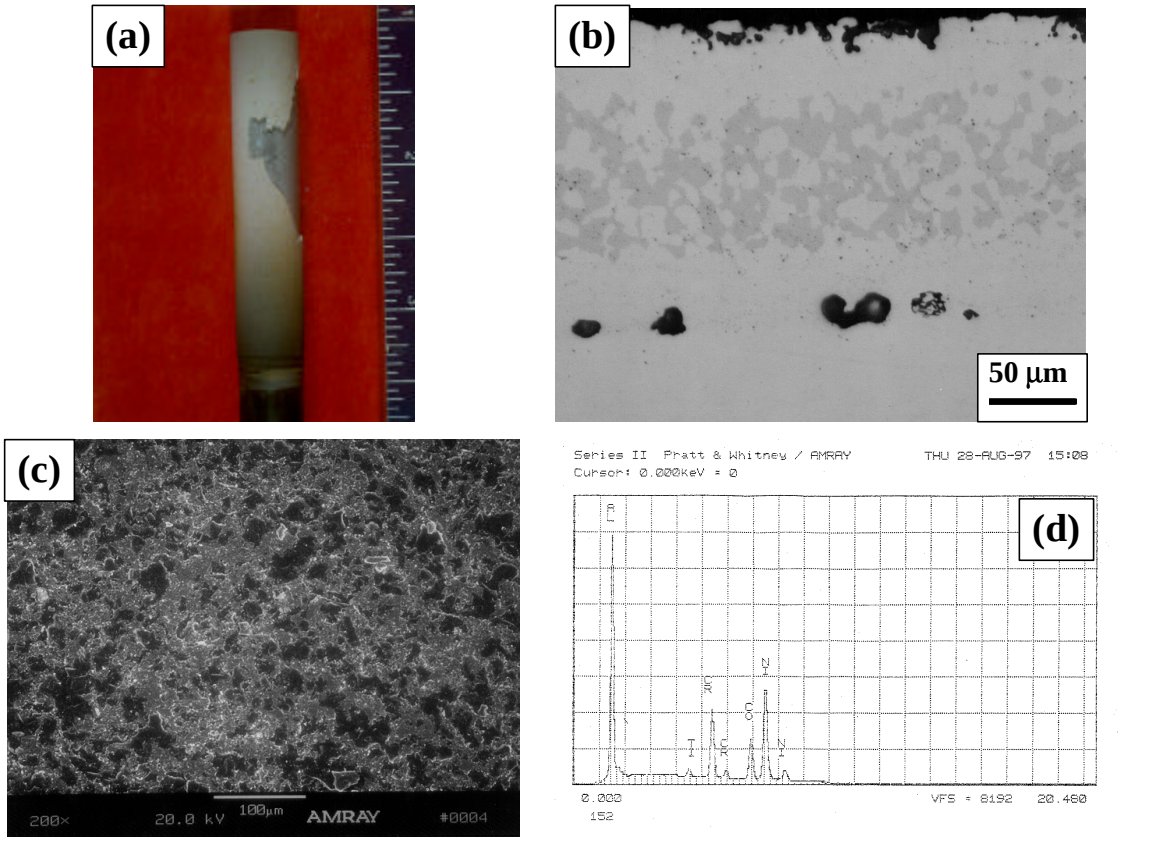

Figure 10. Macroscopic view (a), cross section (b), surface microstructure (c), and the corresponding EDS results (d) for a surface-modified EB-PVD 7YSZ specimen failed in the A2 oxidation test.

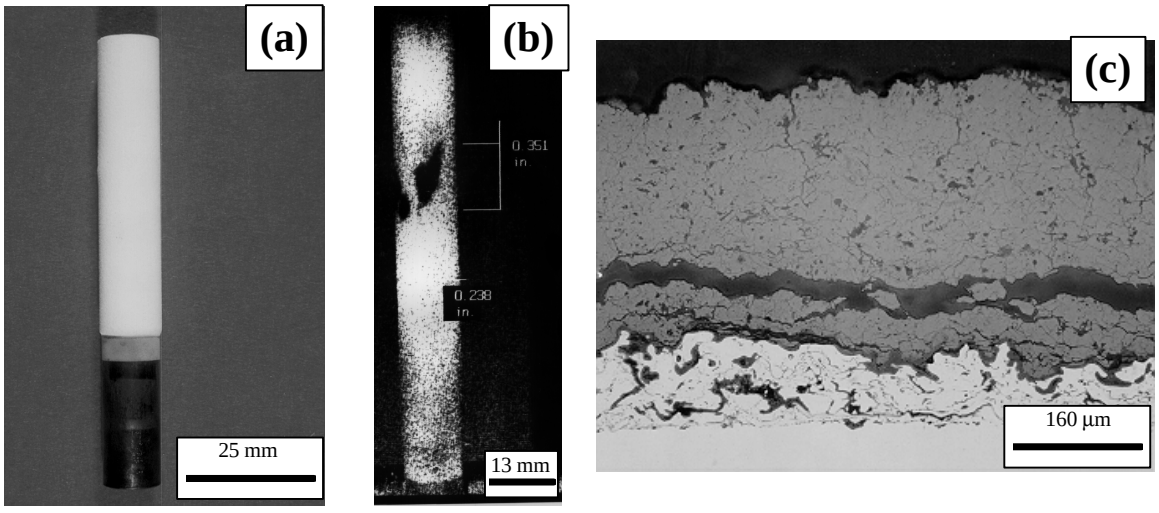

Figure 11. Macrophotograph (a), electronic hologram (b), and the corresponding cross section microstructure (c), demonstrating the capability of electronic holography to nondestructively detect partial TBC delamination.

obtained in the area indicated by the hologram. As seen in Figure 11c, a major crack is detected within the ceramic layer precisely at the location where delamination was expected.

The ceramic erosion test was conducted at 1093°C (2000°F), using quartz or Arizona road dust as erodents (*i.e.*, particulates). Incidence angles of 20° and 90° with respect to the flat specimen surface were employed, with the particulate velocity of 244 or 427 m/s (800 or 1400 fps). The erosion test results for the as-coated, and for the heat-treated (1149°C/100 h) specimens are shown in Figures 12a and b, respectively. Regardless of the absence or presence of a pre-test heat treatment, the surface-modified EB-PVD 7YSZ material was superior to both the standard, state-of-the-art EB-PVD 7YSZ ceramic, as well as to the APS coating.

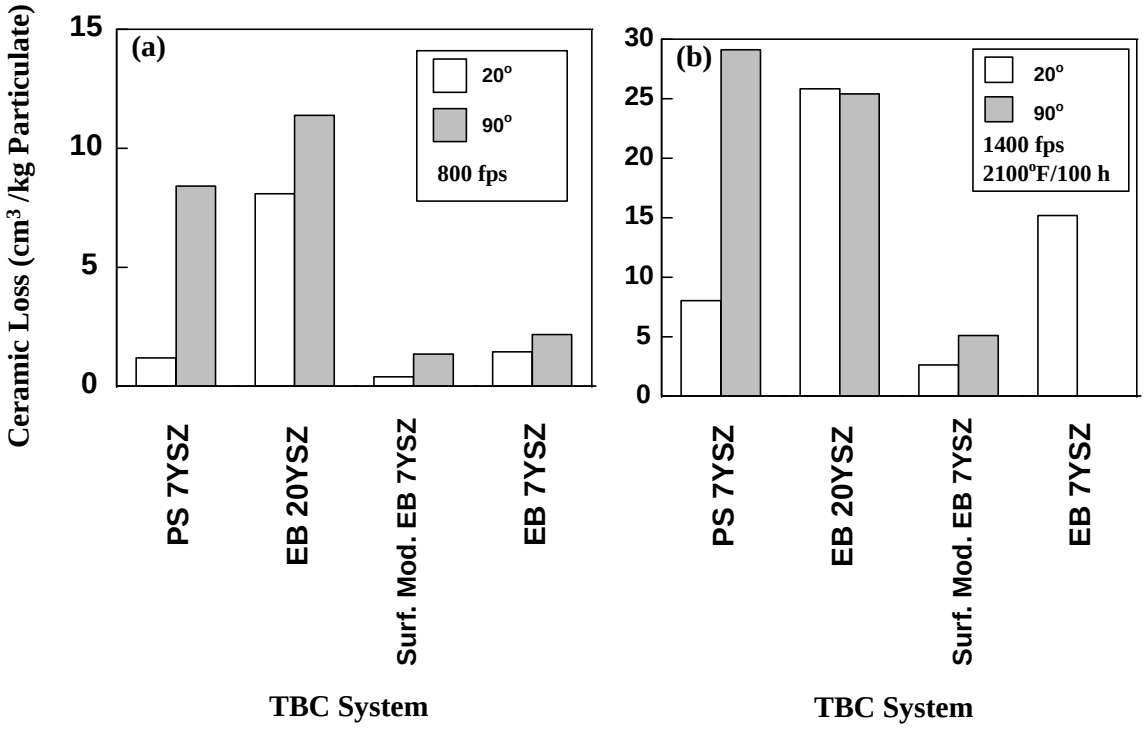

Figure 12. Ceramic erosion test results for the as-received (a) and heat treated (b) candidate materials.

Since the surfaces of ceramic-coated specimens are currently being prepared for the upcoming cyclic hot-corrosion testing in a thermal-gradient burner rig, the hot-corrosion test results are not yet available for review in this paper. However, based on the cyclic oxidation and erosion test data presented above, the surface-modified EB-PVD 7YSZ is considered to be the leading down-select ceramic candidate in this program.

TBC Analytical Modeling Results

An analytical TBC life prediction model is required to reduce engine design risk and define hot-section components overhaul requirements. In the current program, therefore, experimental and computational efforts are focused on developing a design-capable analytical model for IGT applications that captures the physical mechanisms controlling the TBC durability. To develop the model, an approach has been adopted wherein a combination of experimental results, analytical parametric studies and literature information is used. A wide variety of TBC properties and design issues that must be addressed and correlated in the modeling effort are summarized in Figure 13. The properties directly measured and modeled in this program are shown in green, whereas those adopted primarily or exclusively from the literature data for application in the currently developed model are shown in yellow and red, respectively. In this paper, only the effect of ceramic sintering on thermal conductivity is briefly reviewed.

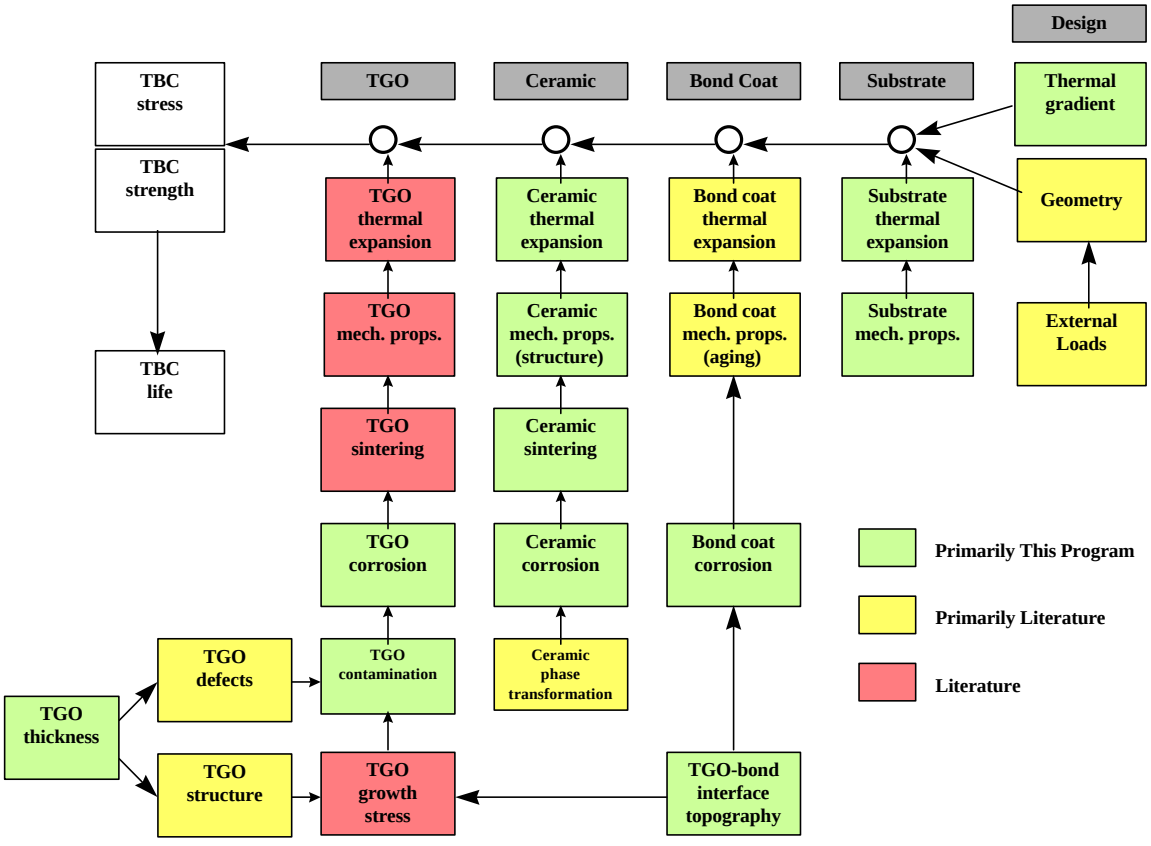

Figure 13. Preliminary TBC life prediction material property requirements.

Experimentally determined values of thermal conductivity for the APS 7YSZ ceramic are compared to the model prediction in Figure 14. The shape of the measurement-temperature dependency of the data is very well described by the 3rd order polynomials shown, whereas the data shift along the vertical axis due to the time/temperature effects

of pre-test heat treatment is well captured by the sintering strain e_s *(t, T)*. It is of interest to note that the presence of corrodent salts and sintering agents in the APS specimen heat treated for 20 h at 1250°C (2282°F) did not affect the thermal conductivity beyond the extent predicted from a simple (contaminant-free) time-at-temperature exposure.

Experimental results and model predictions for the EB-PVD 7YSZ ceramic are compared in Figure 15. In this case, in the temperature range of interest to IGT applications (between 400° and 1200°C, or 752° to 2192°F), the model is fairly effective in predicting the thermal conductivity behavior, but only for the as-received and the contaminant-free heat-treated specimens. Contrary to the results obtained from the APS specimens, the experimental values for the EB-PVD specimen heat treated at 1250°C for 20 h in the presence of corrodents and sintering agents were nearly identical to those measured on the contaminant-free EB-PVD specimen pre-exposed at 1400°C (2552°F) for 10 h. This observation suggests that, in addition to a simple time-at-temperature exposure, the contaminant sulfates and oxides play a role in thermal conductivity behavior of the PVD material. The model consistently underpredicts the results for the 1250°C pre-exposure, which may be related to the ease with which the contaminants penetrate and affect a PVD ceramic microstructure, as discussed above (see Figures 5 and 6).

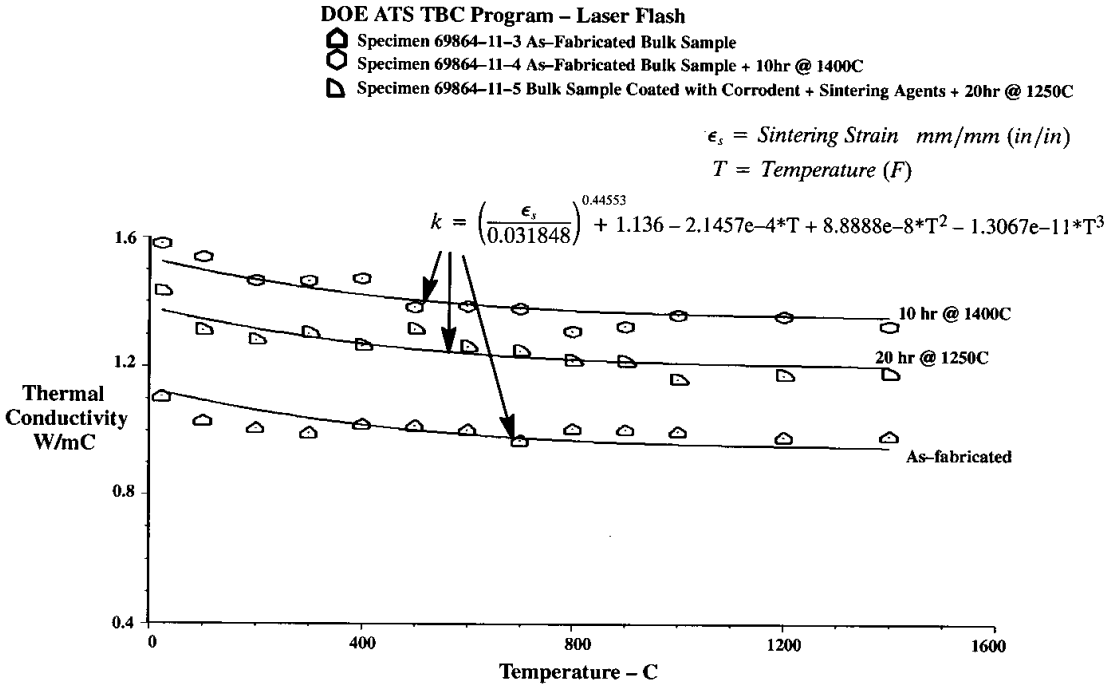

Figure 14. Comparison of measured *vs* predicted thermal conductivity values for the APS 7YSZ ceramic as a function of temperature.

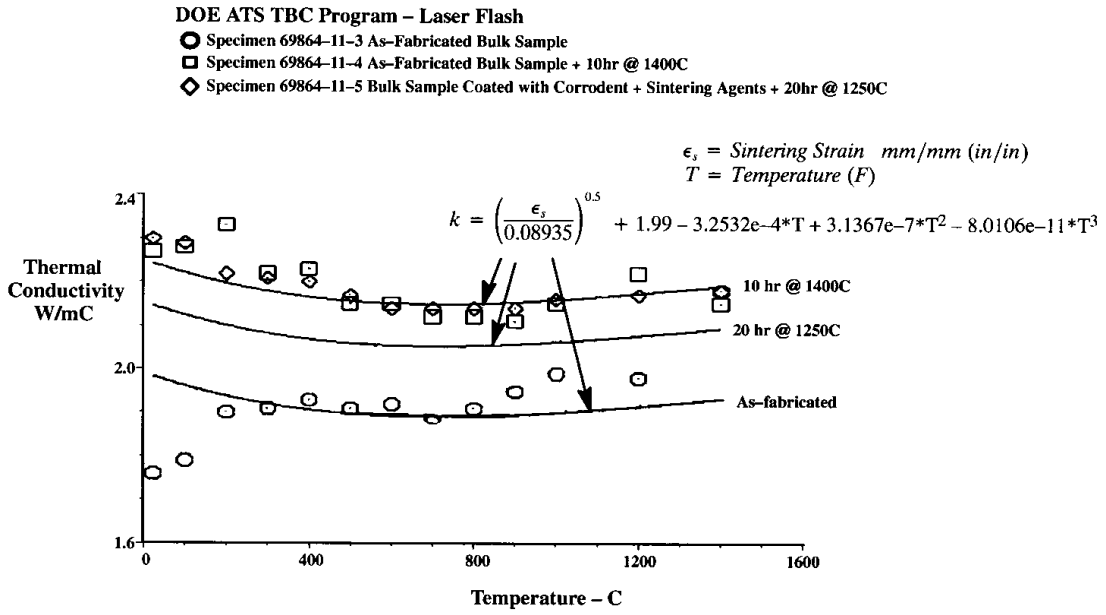

Figure 15. Comparison of the measured vs predicted thermal conductivity values for the EB-PVD 7YSZ ceramic as a function of temperature.

Bond Coat Candidate Materials

Concurrently with the development and downselection of the best ceramic material, both the overlay and diffusion-type bond coat candidates are being investigated for down-selection and further evaluation in combination with the most promising ceramic(s).

Typical as-coated microstructures of overlay bond coats being evaluated in this program are reviewed in Figure 16. The standard, low-pressure plasma sprayed (LPPS) NiCoCrAlY bond coat, used successfully in all Pratt & Whitney flight engines, serves as a base line. The high-chromium and oxide-dispersion strengthened (ODS) materials are being considered to improve the bond coat hot-corrosion resistance. The high-velocity oxy-fuel (HVOF) NiCoCrAlY is being pursued with the objective of reducing the manufacturing cost, while potentially still taking advantage of the beneficial properties provided by the standard LPPS material.

Among the diffusion-type bond coats, modifications to the near-surface layers of the single-crystal IN 792 base alloy are being implemented by additions of platinum and aluminum, with the objective of suppressing the kinetics of nucleation and growth of the transient oxides, while simultaneously promoting the formation of the desired, thermodynamically favored alumina scale. In addition, the aluminum concentration in the modified surface layer is being adjusted to produce the γ, γ', or $\gamma + \gamma'$ phase morphology, thus allowing an improved control of the bond coat mechanical properties as compared to the standard β-type intermetallics that exhibit a ductile-to-brittle phase transition. The resulting microstructures of the surface-modified base alloy are shown in

Figure 17. The high-aluminum specimen has developed a thin (< 0.25 μm), homogeneous oxide scale suitable for subsequent TBC processing (Figure 17a), whereas the low-aluminum specimen has produced a discontinuous, nonuniform and somewhat thicker (> 0.75 μm) oxide layer unacceptable for further development (Figure 17b).

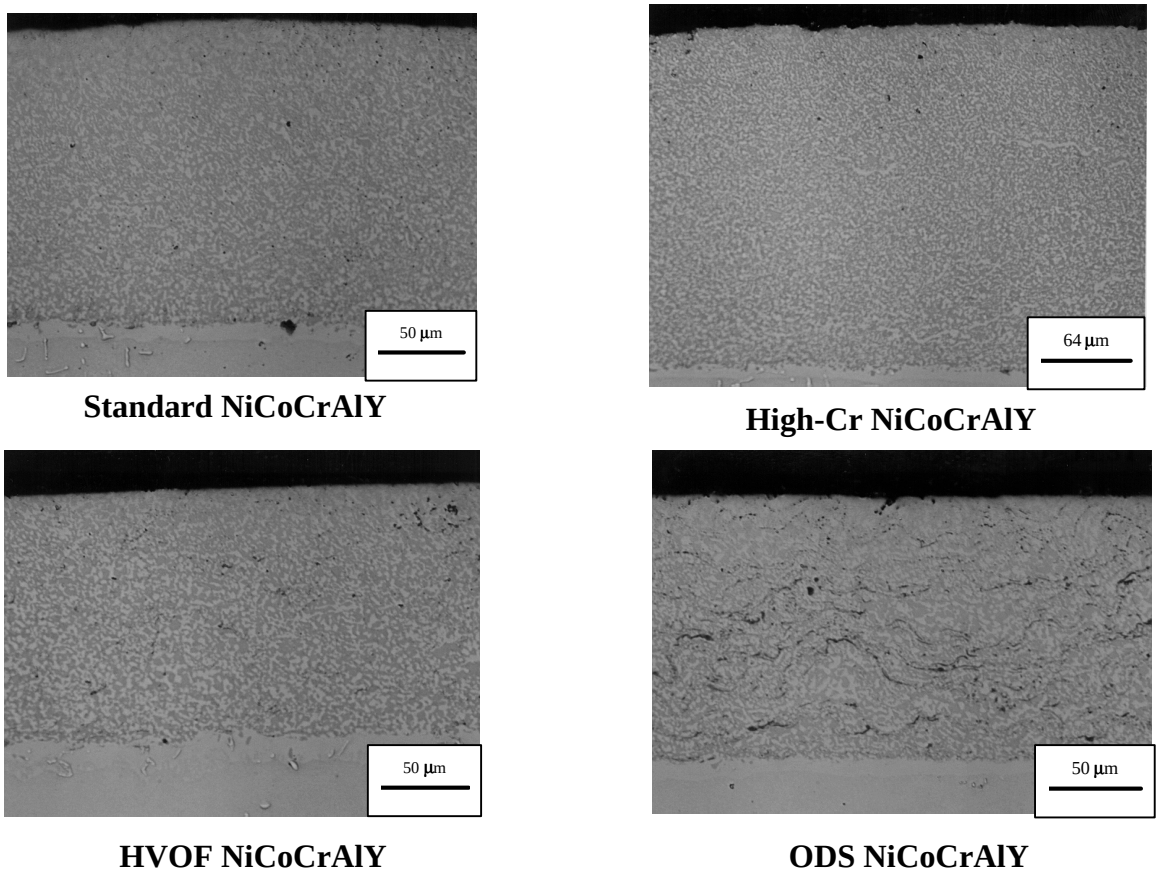

Figure 16. Typical as-coated microstructures of overlay bond coat candidate materials.

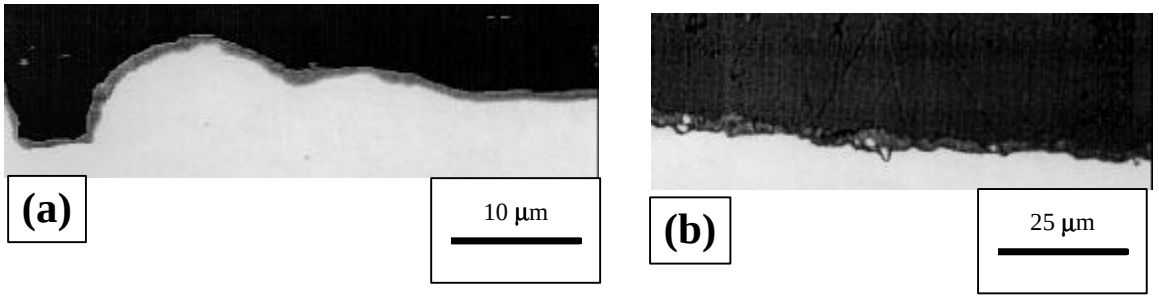

Figure 17. Microstructure of platinum modified single-crystal IN 792 base alloy corresponding to high (a) and low (b) aluminum additions.

Thermal Gradient Burner Rig Test Facility

Thermal gradient in the ceramic is a critical parameter in TBC performance, because it is the source of thermal stress, and, consequently, dictates the component life. In an engine, a high temperature gradient is established across the ceramic due to a high heat flux. In order to simulate the engine conditions as closely as possible, a majority of TBC oxidation and hot-corrosion testing in this program will be conducted in a thermal gradient burner rig, which has been installed and is now fully operational.

The schematic of the rig setup is presented in Figure 18. The power output of the rig is 146.5 kW (~500,000 Btu/h), with a maximum demonstrated specimen surface temperature in excess of 1288°C (2350°F). The setup provides for rapid rotation (200 rpm) and thermal cycling of a multispecimen test assembly (Figure 19a), with the demonstrated heat-up and cool-down transients of 33°C/s (60°F/s) and 100°C/s (180°F/s), respectively. With the cooling air supply of up to 0.23 kg/s (0.5 lb/s) at 5.9 kPa (85 psig), preliminary temperature calibration runs have indicated a temperature gradient of 206°C (370°F) across a 0.254 mm (0.010") thick layer of APS ceramic.

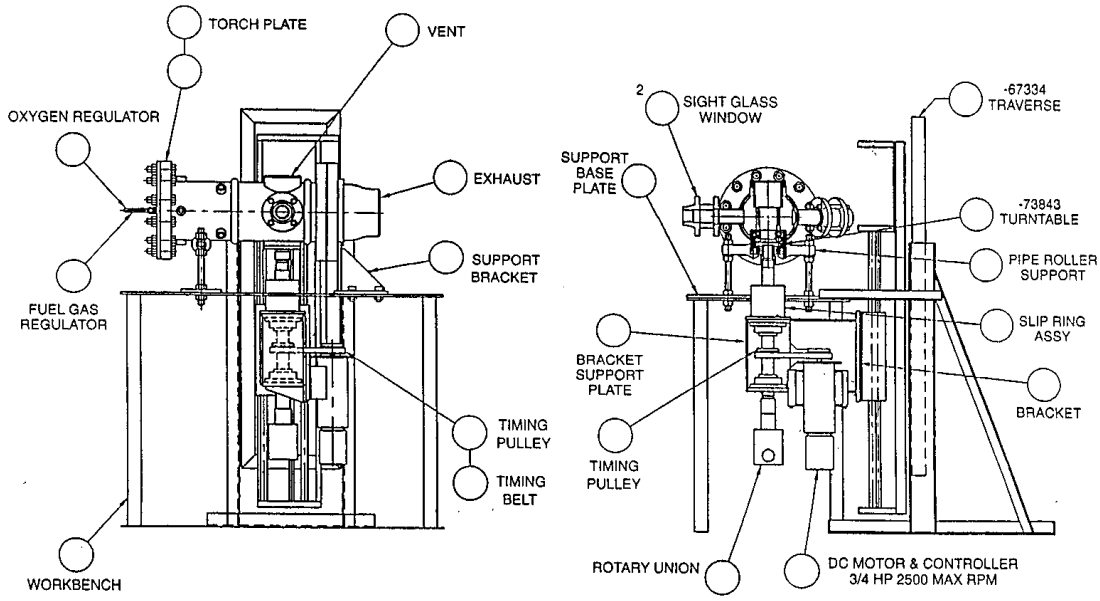

Figure 18. Schematic of the thermal gradient burner rig.

In addition to evaluating the standard cylindrical test specimens shown in Figure 19a, the rig is equipped to accept instrumented TBC coated turbine blades (Figure 19b)—a capability required for successful implementation of Phase III of the Program (see Figure 1). As shown in Figure 20, real-time monitoring of the surface and metal temperatures using one and two-color optical pyrometers and thermocouples, respectively, has been demonstrated in a cyclic test on a TBC coated 1st stage turbine blade.

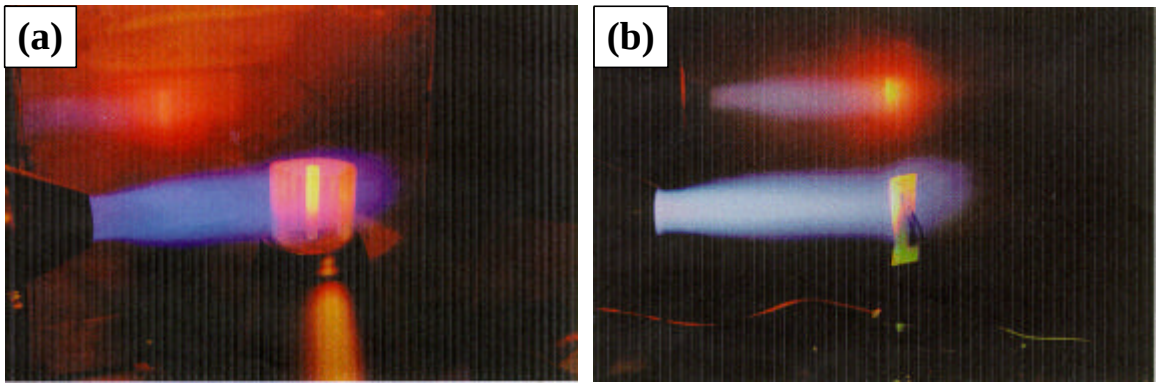

Figure 19. TBC coated cylindrical specimens (a) and a 1st stage turbine blade (b) exposed to a test temperature in the thermal gradient burner rig.

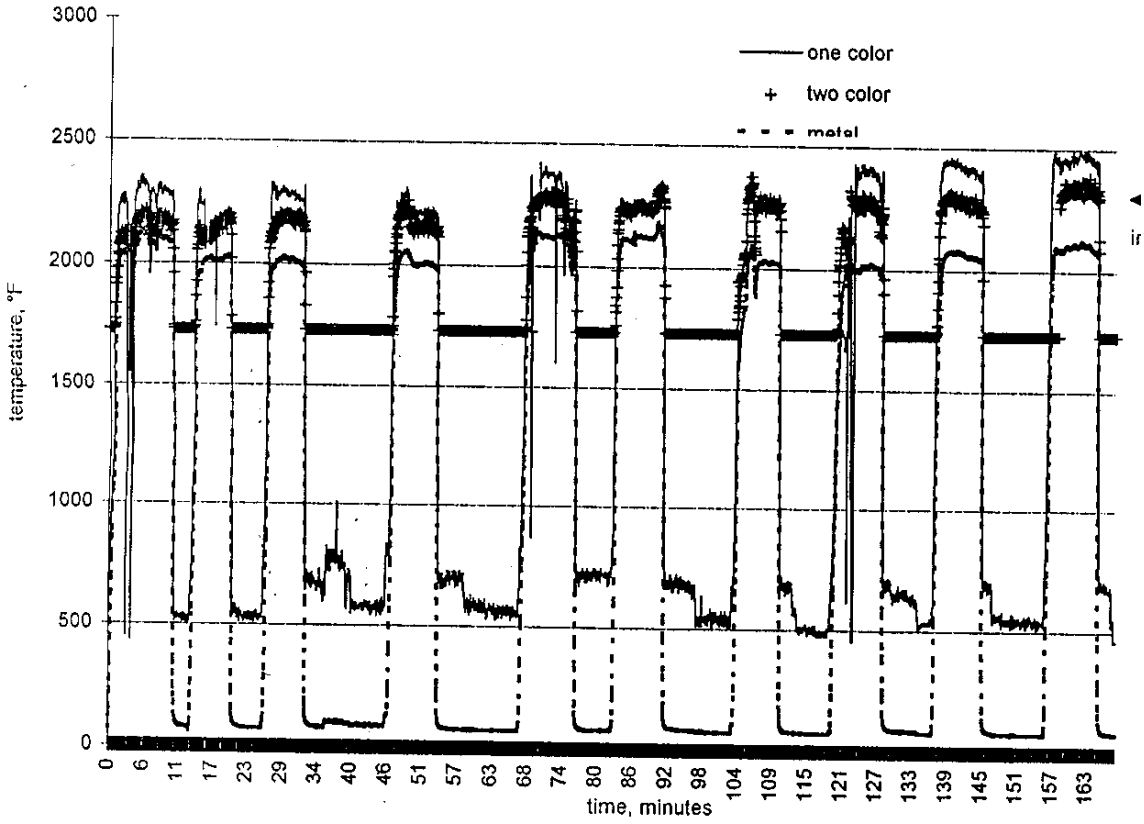

Figure 20. Temperature–time profile for the instrumented TBC coated 1st stage turbine blade (shown in Figure 19b) obtained during a test performed in the thermal gradient burner rig (shown schematically in Figure 18).

Summary—Program Highlights

Following are the highlights of the major technical accomplishments to date:

- Hot-corrosion mechanisms relevant to industrial engine environments have been defined and the surface morphology observed in the field reproduced in the lab.
- Surface-modified EB-PVD 7YSZ has been identified as a leading ceramic candidate for downselection.
- Thermal conductivity model has been correlated to the experimental results obtained from the APS and EB-PVD 7YSZ ceramics.
- Platinum and aluminum additions to the near-surface layers of the single-crystal IN 792 base alloy have produced a homogeneous oxide scale suitable for subsequent TBC processing.
- A thermal gradient burner rig has been installed and component testing capability required for Phase III demonstrated.

Future Activities

The remaining activities on this program include gradient burner rig oxidation and hot-corrosion testing of ceramic candidates, standard burner rig hot-corrosion testing of the bond coats, gradient burner rig hot-corrosion testing of two downselected TBC systems, and gradient burner rig hot-corrosion testing of the final downselected TBC on a 1st stage turbine blade.

References

[1]Report to Congress: Comprehensive Program Plan for Advanced Turbine Systems. U. S. Department of Energy, Washington, DC (1993)
[2]Materials/Manufacturing Plan for Advanced Turbine Systems Program. U. S. Department of Energy, Washington, DC (1994)
[3]Research and Development of Thermal Barrier Coatings Technology—Advanced Turbine Systems: Volume II—Technical. Pratt & Whitney Proposal No. CEB-94A-3668. East Hartford, CT (1994)
[4]N. S. Bornstein, "Reviewing Sulfidation Corrosion—Yesterday and Today," *J. Metals,* **48** [11] 37-39 (1996)

Contract Information

Research sponsored by the U. S. Department of Energy's Oak Ridge Operations Office under Contract No. DE-AC05-95OR22426 with Pratt & Whitney (Jeanine T. D. Marcin–

Program Manager), 400 Main Street M/S 114-41, East Hartford, CT 06108; Phone No. (860) 565-4784, Telefax No. (860) 565-5635, E-mail: marcinj@pweh.com.

Acknowledgments

We would like to acknowledge the keen interest, guidance, and assistance provided by the U.S. DOE and ORNL personnel Patricia A. Hoffman, Debbie Haught, Michael A. Karnitz, Ian G. Wright, Mary H. Rawlins, and Bob Harrison.